

Fast Particle Instabilities in MAST

S.D. Pinches 1), L.C. Appel 1), I.T. Chapman 1), G. Cunningham 1), D. Dunai 2), M.P. Gryaznevich 1), A.R. Field 1), M.J. Hole 3), D.F. Howell 1), M.-D. Hua 4), M.K. Lilley 4), R. Martin 1), S. Saarelma 1), S.E. Sharapov 1), H. Smith 5), R.G.L. Vann 6), S. Zoletnik 2) and the MAST and NBI Teams

- 1) Euratom/UKAEA Fusion Association, Culham Science Centre, Abingdon, OX14 3DB, UK
- 2) RMKI-KFKI, Konkoly Thege Miklós út 29-33, H-1121 Budapest, Hungary
- 3) Research School of Physical Sciences and Engineering, ANU, ACT0200, Australia
- 4) The Blackett Laboratory, Imperial College, London SW7 2BZ
- 5) Department of Physics, University of Warwick, Gibbet Hill Road, Coventry, CV4 7AL, UK
- 6) Department of Physics, University of York, Heslington, York, YO10 5DD, U.K.

E-mail contact of main author: Simon.Pinches@ukaea.org.uk

Abstract: In MAST the population of fast ions created by the neutral beam injection system is super-Alfvénic and both the normalised fast ion pressure, β_f , and the ratio of fast ion energy content to thermal energy content are *in excess* of the values expected in DEMO for fusion born α -particles, thus allowing interpolation (and not extrapolation) of the parameter space for fast particle effects. Measurements of the co-located orthogonal (B_R , B_Z , B_θ) magnetic field components in the frequency range up to 10 MHz have allowed the identification of the polarisation of modes excited with super-Alfvénic NBI ions in the ion cyclotron frequency range. This has led to modes observed at around the on-axis cyclotron frequency being identified as compressional Alfvén eigenmodes. Their toroidal mode numbers, n , have been measured to lie in the range $4 < |n| < 10$ and they have been simultaneously observed to propagate both co and counter to the plasma current. These modes usually appear separated in discrete frequency groupings, with the frequency splitting occurring on up to three frequency scales. Nonlinear frequency sweeping of the modes has also been observed in accord with hole-clump formation. 1-D and 2-D models have been developed to further investigate the linear stability and spectrum of these modes. They indicate that the modes are localised at approximately half the minor radius and explain why negative toroidal mode numbers can be driven by the beam ion distribution via the Doppler-shifted cyclotron resonance. In order to investigate the spectrum of Alfvén eigenmodes in high β plasmas, MAST has recently installed a 12-coil TAE excitation system capable of measuring the spectra of stable modes in the system and a subset of three coils has detected modes in the toroidal and ellipticity induced Alfvén eigenmode frequency ranges to have damping rates comparable to the values found on other devices such as JET.

1. Introduction

Fusion produced α -particles possess super-Alfvénic velocities and thus the potential to drive Alfvénic instabilities, which is why one of the most important new problems to be assessed for ITER and DEMO is that of fast particle stability. MAST is well placed to address questions regarding the linear stability and key nonlinear regimes of Alfvénic instabilities since MAST's dimensionless parameters, $v_{\text{fast}}/v_A \sim 2.4$, and $\beta_{\text{fast}}/\beta_{\text{th}} \sim 50\%$ are close to, or in excess of, those expected for ITER or DEMO. The very broad range of parameters achievable on MAST makes it possible to investigate whether systems with high β plasmas possess advantages in terms of confining fusion produced α -particles. One such area of interest is the study of the dramatic changes in the shear-Alfvénic spectrum at high values of β as expected theoretically [1] and found experimentally in MAST [2]. The key difference between MAST and ITER is the ratio of fast ion orbit width to plasma minor radius. However, this should mean that MAST will likely overestimate fast ion transport properties due to Alfvénic modes, providing conservative physics constraints for future machine design.

1. Compressional Alfvén Eigenmodes

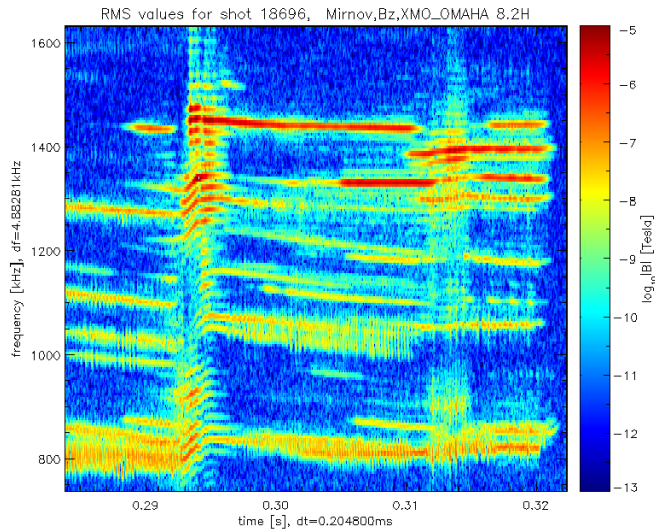


Figure 1: Magnetic spectrogram showing mode activity at frequencies up to 1.6 MHz in MAST #18696

High-frequency activity in the frequency ranges $0.3 < \omega/\omega_{ci} < 0.6$ and $\omega/\omega_{ci} \sim 1$ was first reported on the spherical tokamak START [3]. These modes, driven by super-Alfvénic beam particles were subsequently also observed on NSTX [4] and DIII-D [5] and were identified as Compressional Alfvén Eigenmodes (CAE's). Frequent observations of CAE activity have been made in MAST discharges with neutral beam power exceeding 1.5 MW and where the beam ions are super-Alfvénic, $v_b/v_A > 2$ [6,7]. Figure 1 shows high frequency mode activity in MAST #18696. This is a robust and repeatable deuterium scenario ($B_T = 0.5$ T, $I_p = 700$ kA, $n_e = 3.3 \times 10^{19} \text{ m}^{-3}$) with approximately 2 MW of neutral beam heating present. The modes are observed to lie in the frequency range between $\omega_{ci}/4$ and $\omega_{ci}/2$, where ω_{ci} is the on-axis deuterium ion cyclotron frequency. A frequency sweeping regime was found to be characteristic for the modes at around 800 kHz in this pulse, with hole-clump pairs interpreted as being responsible, as previously inferred for the frequency evolution of lower frequency TAEs in MAST [8] and also for high frequency modes on MAST [6] and NSTX [9]. The toroidal mode numbers, n , have been measured to lie in the range $4 < |n| < 10$ and have simultaneously been observed to propagate both co ($n > 0$) and counter ($n < 0$) to the plasma current. A recent analysis of the mode frequency separation in such discharges [10] has provided evidence that the fine-scale-splitting is in some cases a result of non-linear coupling with a low-frequency global mode. Figure 2 shows the comparison of data with a non-linear model in which a single $(m,n) = (1,1)$ at 16 kHz is driven to fifth-order in non-linearity, interacting with a single high-frequency $n = 8$ mode at 290 kHz. The nonlinear coefficients are determined by fitting to the five discernable low frequency peaks. The n number of the low frequency side-bands is correctly predicted by the nonlinear model, as is the frequency, mode number and side-band amplitude of the $n = 8$ CAE activity. Gaussian noise has been added to the fitted signal with $\sigma = 0.001$ V. A systematic bi-coherence provides further confidence that the

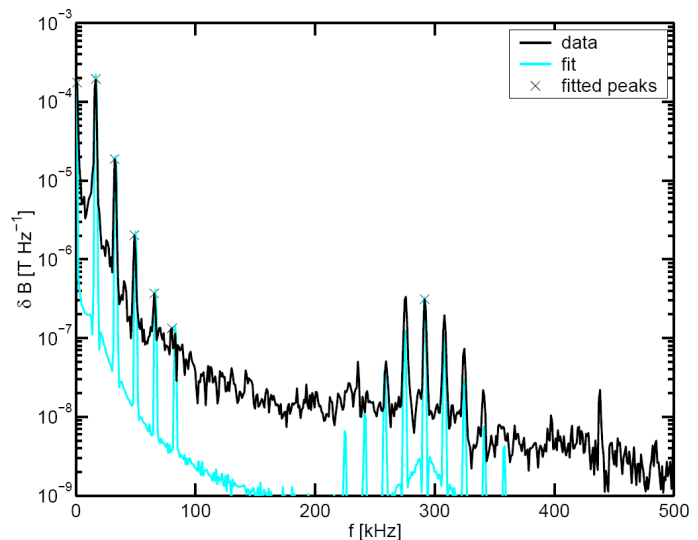


Figure 2: Spectrum of MAST #9429 at 220 ms with predictions of nonlinear model overlaid.

observed high-frequency modes are non-linearly coupled [10]. Radial flux surfaces can be found such that the general frequency evolution of each of the modes follows the local Alfvén frequency upon the surface [6].

1.1 Polarisation

In order to demonstrate that these modes are compressional Alfvén waves and not shear Alfvén waves, i.e. their perturbed parallel magnetic field, $\delta B_{\parallel} \equiv \delta \mathbf{B} \cdot \mathbf{B}_0 / B_0$, is not small compared with their perturbed perpendicular magnetic field, $\delta B_{\perp} \equiv |\delta \mathbf{B} \times \mathbf{B}_0| / B_0$, the polarisation of these modes has been investigated [6,11]. The polarisation of these modes was calculated using measurements of the three orthogonal components of the magnetic field (B_R, B_Z, B_{ϕ}) at the same spatial position. Figure 3 plots $\mathbf{e}_n \cdot \mathbf{B}_0$ at $R = 1.7$ m, $z = 0.2$ m, $\phi = 306^\circ$ where \mathbf{e}_n is a unit vector normal to the plane of polarisation for MAST discharge 17944. The results show that $\mathbf{B}_0 \cdot \mathbf{e}_n$ is significantly smaller for the high-frequency modes compared to the low-frequency activity. Both low and high frequency modes are elliptically polarised.

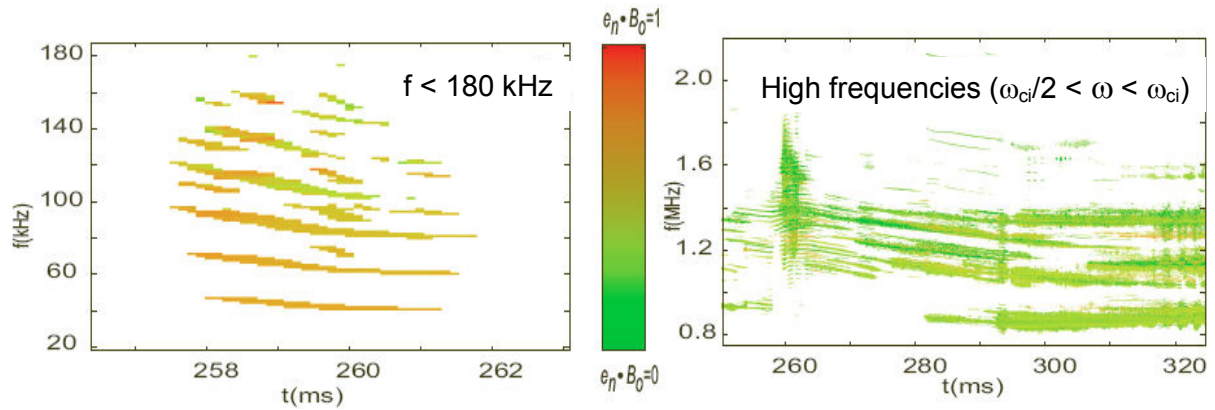


Figure 3: Orientation of polarisation plane for low and high frequency modes in MAST #17944

Measurements from other discharges confirm the general result $|\mathbf{e}_n \cdot \mathbf{B}_0| < |\mathbf{e}_n \times \mathbf{B}_0|$ for high frequency modes; in contrast lower frequency activity such as TAEs and tearing modes exhibit $|\mathbf{e}_n \cdot \mathbf{B}_0| > |\mathbf{e}_n \times \mathbf{B}_0|$. These results provide strong supporting evidence that the high frequency modes are CAEs, although a full interpretation of the results requires the calculation of the variation of the polarisation with radius to confidently interpret them.

1.2. Mode Structure

The spatial structure of CAEs has previously been studied both analytically and numerically. The analytical works suffered from several limiting assumptions that were necessary in order to make the problem tractable [12,13], in particular that $k_{\parallel} \ll 1$ and $\omega/\omega_{ci} \sim 1$. The numerical approaches have either not been suitable for large ellipticity tight aspect ratio plasmas [14], or do not include the Hall term [15]. Recently, the structure has been studied by solving the linearised cold plasma Hall-MHD equations numerically [16] for a particular toroidal mode number. The experimentally observed frequency is typically around half the ion cyclotron frequency, so the Hall term needs to be included. A low β assumption is made, in order to exclude the slow magnetoacoustic mode and to be able to use the cold plasma model. For a spherical tokamak it is also important to treat the variation of the equilibrium magnetic field correctly. Moreover, the parallel wavenumber k_{\parallel} is allowed to be non-zero, but assumed to be small enough to avoid coupling to the shear Alfvén branch ($k_{\parallel} \ll \omega/v_A$). The calculated eigenmodes possess all the main characteristics of CAEs, namely: the perturbed magnetic field is dominantly polarised in the direction of the equilibrium field (i.e. parallel); the modes

are localised in the outboard region; and the mode frequencies are in the ion cyclotron frequency range. Figure 4 shows examples of the calculated eigenstructures of CAEs in a poloidal cross-section through a MAST plasma. The calculations were based on a typical

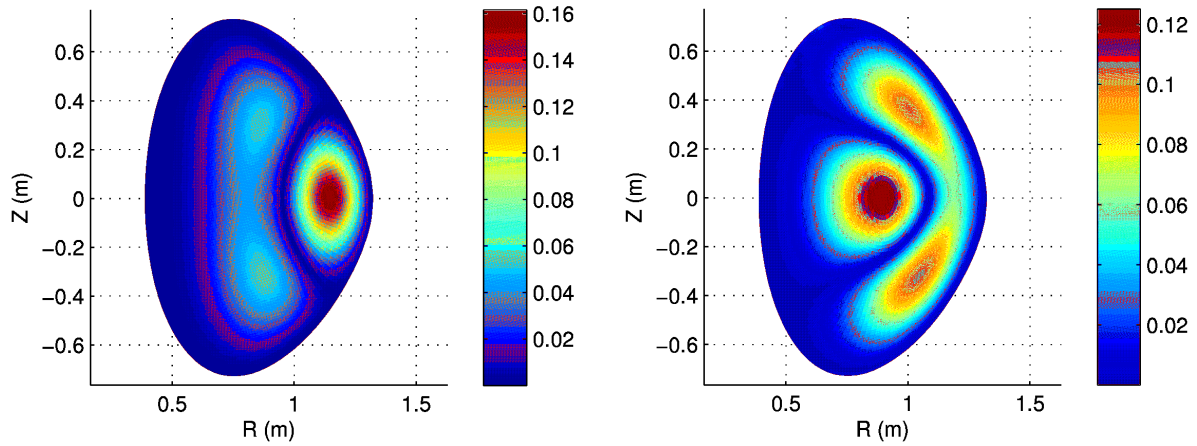


Figure 4: The magnitude of the parallel magnetic field component $|b_{||}|$ for $n = 3$ solutions with $f = 1.56$ MHz (left) and $f = 1.74$ MHz (right) [16]

MAST equilibrium, #18696, reconstructed using the CHEASE equilibrium code [17] with $B_T = 0.47$ T on the magnetic axis and $I_p = 790$ kA, together with a parabolic density profile with the on-axis value $n = 3.5 \times 10^{19} \text{ m}^{-3}$. For the CHEASE equilibrium the ion cyclotron frequency varies from 2.4 MHz on the outboard side to 7.4 MHz on the inboard side. A perfect conductor boundary condition was used for the calculation in Figure 4, which shows two solutions with different eigenfrequencies for $n = 3$. Solutions for the high n modes observed in MAST experiments are not easily found. The mode on the left is radially localised at $r/a \sim 0.5$ in agreement with the location where the local Alfvén frequency was found to linearly scale with the mode frequency [6].

1.3. Linear Stability

A 1-D eigenmode model with finite $k_{||}$ has been developed to allow the effects of various plasma parameters upon CAE modes to be investigated [18,19]. This model is simpler than other models [12,20], but allows extensive parameter scans of toroidal mode number and $k_{||}$ and utilises the NBI fast ion distribution functions computed using the TRANSP code [21]. The model indicates that the modes are localised at approximately half the minor radius and show significant compressional polarisation (in accordance with the observations). It also describes the change in polarisation with radius, as well as indicating via the resonance condition, why negative toroidal mode numbers are preferentially driven by the experimental beam ion distribution function. For instabilities with frequency ω comparable to the ion cyclotron frequency ω_{ci} , the relevant fast particle resonance responsible for the mode excitation is the Doppler shifted cyclotron resonance [22],

$$\omega - k_{||} v_{||\text{res}} - l \omega_b = 0 \quad (1)$$

where $k_{||} = \mathbf{k} \cdot \mathbf{B}_0 / |B_0|$, l is an integer, $l = +1$ corresponds to the Doppler resonance, $l = -1$ corresponds to the anomalous Doppler resonance, $v_{||\text{res}}$ is the parallel velocity of the resonant beam particles and ω_b is the beam ion cyclotron frequency. Note on MAST the NBI and thermal plasma ions are both deuterium so that $\omega_b = \omega_{ci}$. Using TRANSP with 5×10^5 macro particles the deuterium NBI distribution function during CAE activity has been calculated, which shows that most of the NBI produced ions are deposited in the core. Figure 5 shows that a bump-on-tail in the NBI distribution exists at high energy out to a normalised radius of

$r/a = 0.425$, where $n_0 = 4 \times 10^{19} \text{m}^{-3}$, $T = 950 \text{eV}$, $n_b = 5 \times 10^{17} \text{m}^{-3}$. A 1-D ‘hollow cylinder’ model of the plasma equilibrium in a spherical tokamak [19] is used for calculating the discrete spectrum of AEs in the frequency range compatible with the experimental observations. The Doppler resonance condition given in Eq. 1 is used to identify the resonant particle velocity for a given eigenmode. As a result of the eigenmode analysis, $E(r)$ is obtained for use in global drive calculations. The observed $n < 0$ modes were driven via the Doppler resonance, $l = +1$ in Eq. 1, while the $n > 0$ modes can only be driven via the anomalous Doppler resonance, $l = -1$. Although the NBI ions in MAST were super-Alfvénic, they were just below the critical beam speed required for exciting the right hand polarised compressional Alfvén eigenmodes (CAEs),

$$v_{\parallel b} > \frac{3\sqrt{3}}{2} v_A. \quad (5)$$

In the future, the validity of Eq. 5 will be tested experimentally by lowering the magnetic field.

2. Stable Spectra

In addition to its significant capability to study strongly driven fast ion modes, MAST has recently installed and tested a 12-coil active excitation system capable of measuring the spectra of stable modes in the system. Similar systems have been installed and exploited on the conventional aspect ratio tokamaks JET [23] and Alcator C-MOD [24]. Previous results have indicated that as the normalised plasma pressure is increased up to around 10% or more, the spectra of stable modes in a spherical tokamak may be modified; i.e. not only does the damping rate of such modes change, they may even cease to exist as an eigenmode of the system [25]. The principle damping processes are continuum damping [26], radiative damping [27] and thermal ion Landau damping [28]. By actively driving the 6 coils in the lower half of the vessel it is possible to apply dominantly $n = 1, 2$, and 3 perturbing fields. From the external magnetic pick-up measurements at the antenna driving frequency, the plasma’s response to the applied field, and thus the system’s transfer function, may be

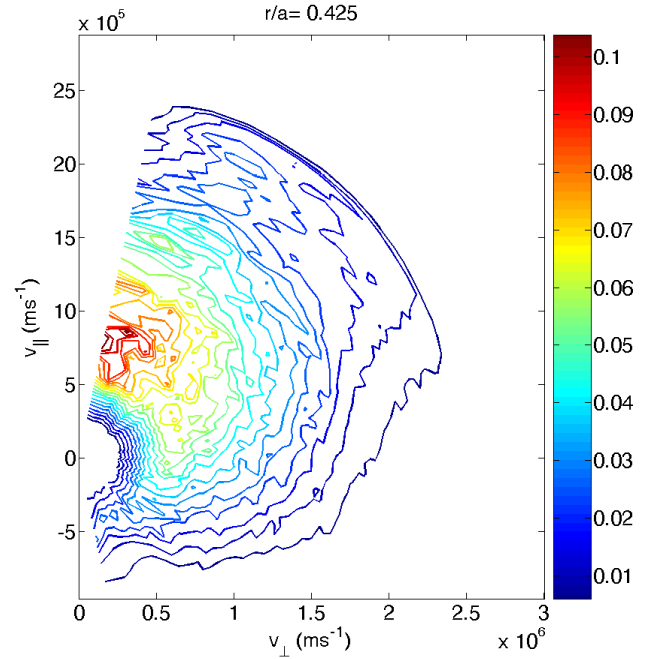


Figure 5: Contours of NBI distribution in $(v_{\parallel}, v_{\perp})$ space showing peak at $v_{\parallel} = 800 \text{ km/s}$, $v_{\perp} = 250 \text{ km/s}$.

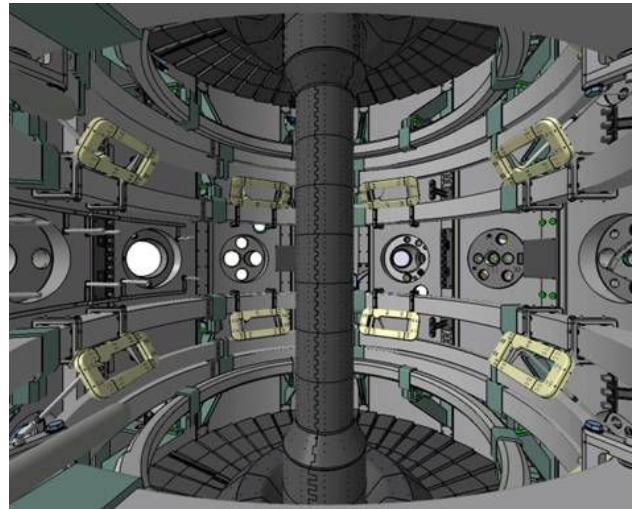


Figure 6: Array of 12 in-vessel coils capable of measuring stable spectrum of modes in MAST

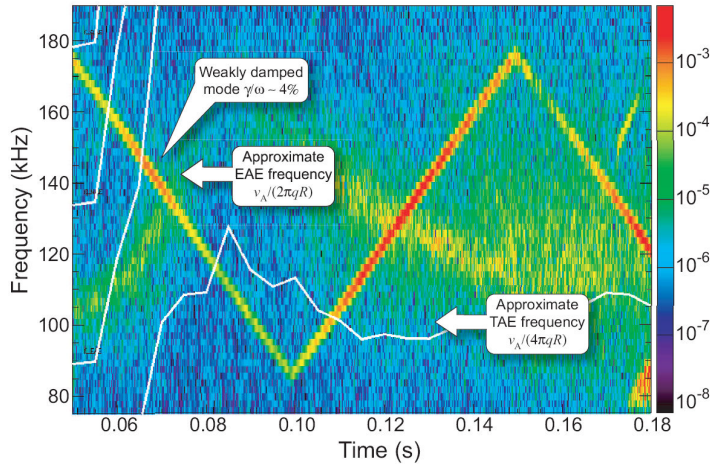


Figure 7: Spectrogram from outboard magnetic coil showing frequency sweeping of active antennas in #18487

Alfvén eigenmodes ($f \sim \nu_A/4\pi qR - \nu_A/2\pi qR$). An analysis of this case performed assuming a single stable mode excited by each antenna sweep, inferred a stable mode at around $t = 65$ ms and $f = 140$ kHz to have a damping rate, $\gamma_d/\omega \sim 4\%$ and at $t = 125$ ms, $f = 130$ kHz to have a damping rate, $\gamma_d/\omega \sim 20\%$. The first value is comparable to that found on other devices such as JET [23], whereas the second is larger and is interpreted as several closely spaced modes which cannot be resolved individually in this case due to the antenna frequency sweep rate.

3. Long-lived Mode

Recent NBI heated MAST discharges, such as #18501 shown in Figure 8, often show frequency sweeping $n = 1$ modes that evolve into a long-lived saturated mode whose frequency evolution tracks the central rotation frequency measured by charge exchange (white points). Analysing the vertical and horizontal soft X-ray arrays reveals that the mode has an internal kink-like structure. Following the transition from the characteristic fishbone-like behaviour, a reduction in both ion and electron densities and temperatures is measured. The plasma rotation also monotonically decreases from the start of the frequency chirping events despite the heating power from the two NBI sources remaining constant (3.5 MW) throughout the pulse. Simultaneous counter-viewing bolometer measurements show a significant increase, consistent with an enhanced level of fast ion losses. A TRANSP analysis for this shot with no anomalous fast ion diffusion predicts a neutron rate approximately twice as high as observed, also consistent with a loss of fast ions and this mode being responsible for a degradation in plasma confinement. This long-lived

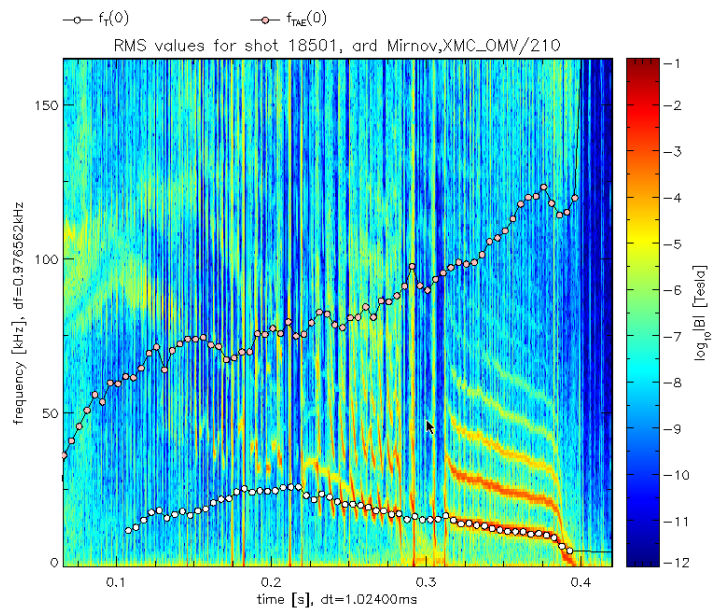


Figure 8: Fourier spectrogram of outboard mid-plane magnetic probe measurement in MAST #18501.

determined. An iterative fitting procedure to the functional form of the transfer function expected for a single mode resonance [29] is then used to determine the damping rates of the observed resonances. Figure 7 shows a spectrogram generated from an outboard magnetic pick-up coil showing the plasma response to perturbations applied using only three active coils located at 15° , 75° and 195° in the frequency range 80 – 180 kHz. The figure shows how the antenna sweeps across the characteristic frequencies associated with toroidal and ellipticity induced

steady-state saturated mode thus offers an excellent opportunity to study fast particle transport effects due to fast ion driven modes.

4. Internal Fluctuation Measurements

The magnetic diagnostics installed on MAST are digitised such that modes with frequencies up to 5 MHz can be studied. However, within the nuclear environment of a burning plasma, high frequency magnetic measurements may no longer be possible due to the blanket requirements. Alternative diagnostics capable of providing information on the perturbations present have therefore been investigated on MAST. Figure 9 presents a comparison of fast particle driven chirping modes excited in MAST #18501 and observed on several systems, namely the array of magnetic probes, the soft X-ray diagnostic and in beam emission spectroscopy (BES) measurements. The latter two diagnostics are not only identified as alternatives to external magnetic measurements but may also provide additional important information on the internal structure of the instabilities excited by the energetic ion population or the in-vessel active excitation coils. BES is a localised measurement of density fluctuations derived from D_α emission from the heating beam. The channel depicted views the NBI line of sight at a major radius of $R = 1.31$ m.

5. Conclusions

Recent theoretical and experimental fast particle studies on MAST have extended the domain of instabilities studied up to the ion cyclotron frequency and into the domain of stable modes. High frequency modes in the range 0.4–3.8 MHz and typically with negative toroidal mode numbers have been observed and investigated. The perturbed magnetic field associated with these modes has been measured to be dominantly aligned with the equilibrium magnetic field supporting their interpretation as Compressional Alfvén Eigenmodes. The linearised cold plasma Hall-MHD equations have been solved numerically in two dimensions to provide information on the spatial eigenstructure. A stability analysis has shown that they may be driven by a bump-on-tail free energy source associated with the NBI ions via the Doppler shifted cyclotron resonance condition. The absence of co-propagating ($n > 0$) modes of this type is interpreted to be a result of the existence of a critical beam velocity, which was not exceeded in the experiments performed to date. Fast particle driven $n = 1$ frequency sweeping modes present in NBI heated MAST plasmas have often been observed to transition into steady-state long-lived saturated modes. These modes cause a degradation in plasma confinement as indicated by an accompanying drop in electron and ion densities and temperatures, plasma rotation and neutron rate. Increased bolometer signals provide further

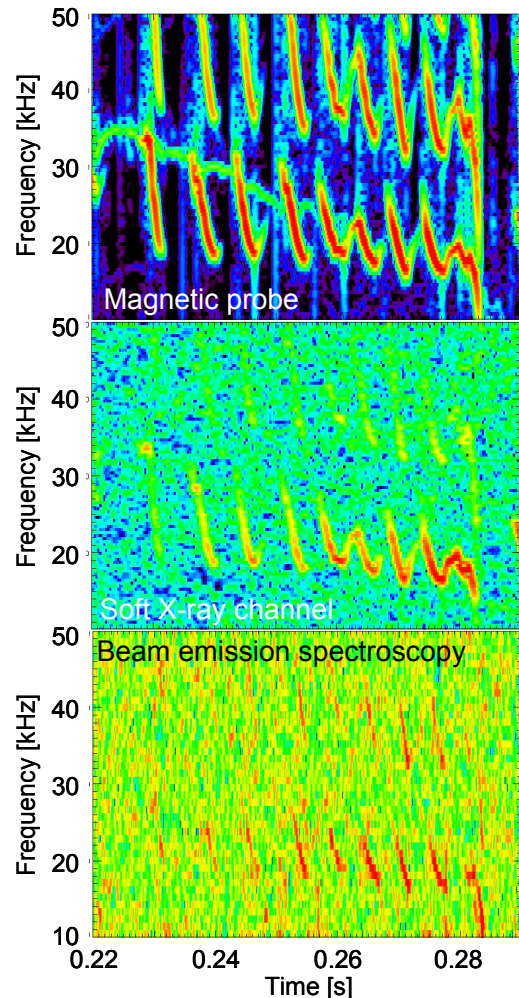


Figure 9: Spectrograms showing fast particle driven chirping modes in #18501: Magnetics (top), soft X-ray (centre), beam emission spectroscopy (bottom).

evidence that this mode causes an enhanced loss of energetic particles. In order to separate the effects of drive and damping a set of 12 coils has been installed in MAST to investigate the properties of the stable spectrum of modes present. The first successful measurements from this new system indicate that the Alfvénic spectrum may consist of multiple closely packed eigenmodes, similar to those observed on JET [30]. In preparation for devices requiring blanket technologies which prohibit the use of high frequency magnetic coils, alternative internal fluctuation diagnostics have been investigated on MAST. In particular, beam emission spectroscopy measurements, soft X-rays and interferometer measurements of the density fluctuations have all been used to observe fast particle driven modes.

This work was partly funded by the United Kingdom Engineering and Physical Sciences Research Council and by the European Communities under the contract of Association between EURATOM and UKAEA. The views and opinions expressed herein do not necessarily reflect those of the European Commission.

References

- [1] FU, G and CHENG, C Phys. Fluids B 2 (1990) 985
- [2] GRYAZNEVICH, M.P. and SHARAPOV, S.E. Plasma Phys. Control. Fusion **46** (2004) S15–S29
- [3] MCCLEMENTS, K. *et al.*, Plasma Phys. Control. Fusion **41** (1999) 661
- [4] FREDRICKSON, E.D. *et al.*, Phys. Rev. Lett., **87** (2001) 145001
- [5] HEIDBRINK, W.W. *et al.*, Nucl. Fusion **46** (2006) 324
- [6] APPEL, L.C. *et al.*, Plasma Phys. Control Fusion **50** (2008) in press
- [7] GRYAZNEVICH, M.P. *et al.*, Nucl. Fusion **48** (2008) 084003
- [8] PINCHES, S.D. *et al.*, Plasma Phys. Control. Fusion **46** (2004) S47
- [9] HEIDBRINK, W. *et al.*, Plasma Phys. Control. Fusion **48** (2006) 1347
- [10] HOLE, M.J. and APPEL, L.C., To be submitted to PPCF (2008)
- [11] VANN, R.G.L. *et al.*, 35th EPS Conf. Plasma Phys. Hersonissos, ECA Vol. 32, P4-064
- [12] SMITH, H., FÜLÖP, T., LISAK, M. *et al.*, Phys. Plasmas **10** (2003) 1437
- [13] GORELENKOV, N.N. *et al.*, Phys. Plasmas **9** (2002) 3483
- [14] HELLSTEN, T. and LAXÅBACK, M., Phys. Plasmas **10** (2003) 4371
- [15] GORELENKOV, N. N. *et al.*, Nucl. Fus. **46** (2006) S933
- [16] SMITH, H. *et al.*, 35th EPS Conf. on Plasma Phys. Hersonissos, ECA Vol. 32, P2-055
- [17] LÜTJENS, H., BONDESON, A., SAUTER, O., Comp. Phys. Comm. **97** (1996) 219
- [18] LILLEY, M. K., Phys. Plasmas, **14** (2007) 082501
- [19] YEGORENKOV, V. D., STEPANOV K. N., 17th EPS, vol. 3, 1207, Venice, 1989
- [20] GORELENKOV, N. N., Nucl. Fusion, **42** (2002) 997
- [21] BUDNY, R., Nucl. Fusion **32** (1992) 429
- [22] AKHIEZER, A. I., Plasma Electrodynamics Vol 1: Linear Theory, Pergamon Press 1975
- [23] FASOLI, A. *et al.*, Phys. Rev. Lett. **75** (1995) 645
- [24] SNIPES, J.A. *et al.*, Plasma Phys. Control. Fusion **46** (2004) 611
- [25] GRYAZNEVICH, M.P. *et al.*, Plasma Phys. Control. Fusion **46** (2004) S15-S29
- [26] BERK, H.L. *et al.*, Phys. Fluids B4 (1992) 1806
- [27] METT, R. and MAHAJAN, S.M., Phys. Fluids B4 (1992) 2885
- [28] BETTI, R. and FREIDBERG, J.P., Phys. Fluids B4 (1992) 1465
- [29] MORET, J.–M., CRPP Report LRP (1994) 498/94
- [30] KLEIN, A. *et al.*, 35th Conf Plasma Physics, Hersonissos, ECA Vol. 32, P5-083